ISSN 1392 - 1207. MECHANIKA. 2009. Nr.1(75)

Mechanical behaviour of reinforced earth retaining walls

L. Belabed*, J. Yahiaoui, A.M. Zennir***, H. Benyaghla******
**University of Guelma, B.P. 401, 24000 Guelma, Algeria, E-mail: drbelabed@yahoo.de*
***University of Guelma, B.P. 401, 24000 Guelma, Algeria, E-mail: djarir2020@yahoo.fr*
****University of Jijel, 18000 Jijel, Algeria, E-mail: abdelmalekzennir@yahoo.fr*
*****University of Guelma, B.P. 401, 24000 Guelma, Algeria, E-mail: hbenyaghla@yahoo.fr*

1. Introduction

The instabilities of slopes constitute always the main risks on human lives and loss of goods. The retaining walls are conceived to retain unstable slopes. There is a large variety of these structures according to the method of their construction and their mechanical behaviour. In 1960, Henri Vidal invents the fundamental mechanism of the reinforced earth and introduced for the first time the "Terre Armée" as an alternative type of the retaining walls ([1, 2]). The reinforcements (metallic strips, geosyntetics, tires, ….) are placed inside the soil mass. The main advantages of the reinforced earth, which explains its significant development in France and worldwide, are its economy, its integration in the ground structures (in the case of road embankments in particular) and especially its great deformability which enables it to adapt without risk to important motions. The reinforcements resist tensile, shearing and/or flexural forces, according to their type, by friction ground-reinforcements. The reinforced earth walls behave mechanically like a weight-wall, using their weight to withstand the earth pressures.

On the basis of full-scale and small-scale tests, we distinguish the following internal failure modes of the reinforced earth retaining walls ([1, 3]):

- failure by break of the reinforcements,
- failure by loss of adherence (pullout),
- failure of the facing,
- overall failure (strip-ground-facing).

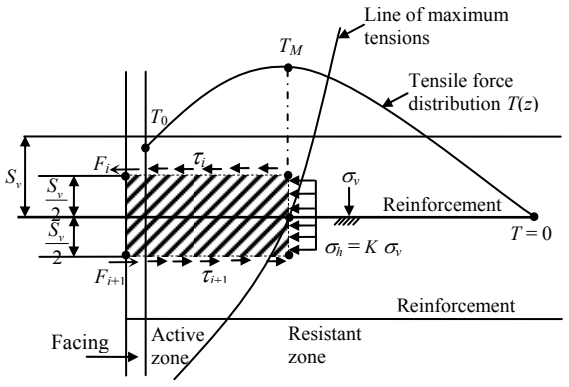

Fig. 1 Principle of the method of local balance

The main aim of this paper is to analyse the latter failure mode (overall failure of the structure). To avoid the overall internal failure (ground-strip-facing), we have to determine the maximum tensile forces developed in the reinforcements and the geometry of the critical slip surface. In this paper, we have studied this type of stability with the traditional method of soil mechanics (limit state equilibrium) [4] and then confronted it with the results of numerical simulation. The general method of checking of the internal stability is summarized in the following steps:

- determine the critical slip surface (mechanical model),
- determine the maximum tensile force on each level of reinforcement,
- determine the maximum tensile force by defect of adherence and by break at each level of reinforcement,
- evaluate the safety factor.

2. Limit equilibrium methods

For all the techniques of the reinforced earth walls, tensile forces in the reinforcements are not maximum at the face but inside the reinforced soil mass. The locus of the points of maximum tension T_{max} separates the soil mass in two zones (Fig. 1): **an active zone** located behind the facing where shear stresses at the interface soil-reinforcement are directed towards the outside and a **resistant zone** where shear stresses are directed towards the interior and are opposed to the side displacement of the active zone ([3, 5-7]).

The method of local equilibrium, which was developed for the first time for the reinforced earth "Terre Armée", consists in studying the equilibrium of a section of ground and facing around a horizontal element of reinforcement (Fig. 1). It is classically supposed that the shear stresses on the upper and lower faces equilibrate as well as the horizontal sharp efforts in the facing. Therefore, the shearing is null at the point of maximum tension T_{max} (T is maximum and its derivative, proportional to τ, is null) and both the horizontal and vertical directions are principal directions for the stresses. The back face of the section is then taken vertical at the point of maximum tension T_{max}, which makes it possible to simply write the horizontal balance of the section in the following form

$$T_{max} = S_v\ S_h\ K\ \sigma_v(z) \tag{1}$$

where S_v and S_h are vertical and horizontal spacing of the reinforcements (Fig. 1); $\sigma_v(z)$ is vertical stress at depth Z and at the point of maximum tension whose distribution along a horizontal reinforcement is supposed to be non uniform (Fig. 1); K is coefficient relating the horizontal stress to the vertical stress, it can be determined as an average coefficient of earth pressure along the line of T_{max} and by the distribution of vertical stress $\sigma_v(z)$ in relation to the depth.

The method of total equilibrium consists of considering plans of potential failure resulting from any point of the facing corresponding to failure wedges (Fig. 2) [3].

3. Mechanical failure models

The stability conditions of a reinforced earth wall are strongly related to the geometry, the properties of mechanical resistance of the ground, the reinforcement and the ground-strip interaction. The principle of the detection of risks of failure is summarized in two steps:

- the objective of the first step is to identify the geometrical configurations favourable to failure for the various known failure mechanisms (plane failure, circular failure and mixed failure),
- the second step implies the calculation of the safety factors associated to each failure mechanism identified at the preceded step.

We assume that the most critical slip surface by a reinforced earth wall coincides with the line of maximum tensile forces (i.e. the locus of maximum tensile force T_{max} in each layer of reinforcements).

In this paper, we have studied three mechanical failure models of reinforced earth retaining walls which are illustrated in Fig. 2.

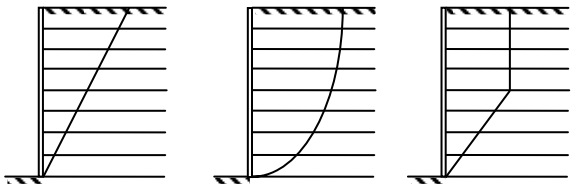

a b c

Fig. 2 Mechanical models of overall failure of a reinforced earth wall: *a* - plane failure, *b* - circular failure, *c* - mixed failure

We cut out the soil mass in a number of elementary volumes (slides), for each of these the line of slip is a straight one, i.e. we discrete the failure surface in segments of equal lengths $S_v/sin\theta$ (Fig. 3) where S_i is vertical component of the forces inter-slides, E_i is horizontal component of the forces inter-slides, W_i is unit weight of the slide, F_i is reaction of the embankment inclined at an angle φ to the normal on the plan, T_i is tensile strength of the reinforcement, θ is angle of the segment of failure to the horizontal, φ is internal friction angle, S_v is thickness of a section (slide).

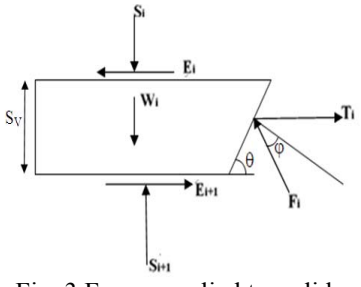

Fig. 3 Forces applied to a slide

To formulate the equilibrium equations corresponding to each of the three mechanical models (slip surfaces) illustrated on Fig. 2, we study the vertical and horizontal balance of an unspecified slide (Fig. 3).

3.1. Plane and circular failure

The mechanical models of plane and circular failures are represented respectively in Figs. 2, a and b. Equilibrium equations of a section of thickness S_v (Fig. 3) can be written:

- projection of forces on vertical

$$W_i + S_i - S_{i+1} - F_i cos\left(\theta - \varphi\right) = 0 \tag{2}$$

- projection of forces on horizontal

$$T_i - E_i + E_{i+1} - F_i sin\left(\theta - \varphi\right) = 0 \tag{3}$$

We make $\Delta E = E_{i+1}$-E_i and $\Delta S = S_i$ -S_{i+1}. From Eq. (2) we have the friction force : $F_i = (W_i+\Delta S)/cos(\theta-\varphi)$, replaced in Eq. (3), we obtain general equilibrium equation for the two slip surfaces cited above

$$T_i + \Delta E - \left(W_i + \Delta S\right) tan\left(\theta - \varphi\right) = 0 \tag{4}$$

We can also calculate tensile force in the reinforcement *i*

$$T_i = -\Delta E + \left(W_i + \Delta S\right) tan(\theta - \varphi) \tag{5}$$

The sum of tensile forces of all the reinforcements cut by the failure surface is in this case equals to:

$$\sum T_i = \sum W_i tan\left(\theta - \varphi\right). \tag{6}$$

3.2. Mixed failure surface

This model is composed of two failure surfaces: one is inclined at an angle θ to the horizontal, it starts from the wall footing and ends at the start of the second failure surface, the latter is vertical and extends up to the upper level of the ground (Fig. 2, c). The procedure of formulation of the limit state equation in this case is quite similar to that for circular and plane surfaces, except that in this case we add earth pressure P_i behind the vertical surface.

The limit equilibrium equation of the mixed failure is written as follows

$$\sum T_i = \sum W_i tan\left(\theta - \varphi\right) + P_i \tag{7}$$

where P_i represents earth pressures behind the vertical failure surface. We have studied in this paper various distributions of the earth pressures (triangular, rectangular, bilinear and elliptic).

The sum of mobilized tensile forces $\sum T_i$ is related to the angle which forms failure surface with the horizontal (θ), the internal friction angle of the ground and the earth pressures (Model of mixed failure).

3.3. Critical failure surface

We have to search iteratively for each of the three models (Fig. 2), the critical slip surface which gives the maximum mobilized resultant of tensile forces $T_{max}=\sum T_i$. For that purpose, the above formulated equilibrium equations Eqs. (6) and (7) are programmed by the authors using

the Delphi language. The software draws the most critical failure model found by iterative calculations and gives information on the crucial angle of failure θ, the maximum tensile force T_i, the resultant of tensile forces $\sum T_i$ and the minimal corresponding safety factor for each model.

To find the most critical mechanical model, we calculate the safety factors against break failure and pull-out failure of the reinforcements [3]

$$F_{S_r} = \frac{T_{max_R}}{T_{max}} \text{ and } F_{S_f} = \frac{T_{max_F}}{T_{max}} \quad (8)$$

where T_{max_F} is maximum tensile force obtained in the case of a pullout failure of the reinforcement; T_{max_R} is maximum tensile force obtained in the case of break failure of the reinforcement.

$$T_{max_F} = 2bf^* \left(\sigma_v + \Delta q\right) L_e \quad (9)$$

$$T_{max_R} = Rba \quad (10)$$

where F_{sr}, F_{sf} are safety factors, respectively applied to tension strength of the reinforcement and to the lateral friction; F_{sr} has a value of 1.5 for ordinary constructions and 1.65 for constructions with high safety level; F_{sf} equals 1.35 for ordinary constructions and 1.5 for constructions with high safety level; b is width of the reinforcement; a is thickness of the reinforcement; f^* is coefficient of apparent friction; σ_v is vertical stress; Δq is additional stress due to a possible overload; L_e is length of the strip in the zone of resistance; R is failure stress of the reinforcement (metallic strip).

In practice, we do not use the coefficient of real ground-strip friction $f = \tau_{max}/\sigma$, but rather a coefficient of apparent friction noted f^* and defined by $f^* = \tau_{max}/\sigma_1$, where τ_{max} is the maximum mobilized shear stress on the face of the reinforcement, σ_1 average vertical stress and σ real vertical stress of the reinforcement [3]. In the case of high adherence steel strips, we have these Eqs. (11) and (12) obtained from experimental results

$$f^* = f_0^* \left(1 - \frac{z}{z_0}\right) + tan\varphi \left(\frac{z}{z_0}\right) \text{ for } z \le z_0 = 6m \quad (11)$$

$$f^* = tan\varphi \text{ for } z \succ z_0 \quad (12)$$

For the embankments in terrestrial site and an angle of friction φ taken equal to the minimal characteristic value of 36°, the coefficient f_0^* depends on many parameters (granularity, internal angle of friction, etc) and it can be evaluated in function of the coefficient of uniformity of the embankment. In absence of precise measurements, we will retain in this paper a value of f_0^*=1.5.

4. Numerical modelling

In this research, the software FLAC^{2d} (Fast Lagrangian Analysis of Continua) based on the method of the finite differences was employed to study the internal stability of the reinforced earth walls [8]. It provides the fields of strains and stresses. The continuous medium is discredited in quadrilaterals, each one of them being divided into two pairs of triangular elements with uniform deformation. The failure criterion used in this work is that of Mohr-Coulomb "elastic-plastic". Boundary conditions are taken into account by blocking horizontal displacement in the direction y and horizontal and vertical displacement for the lower limit (base). The metallic strips are modelled like bars. Input data for the ground, steel strips and interface are summarized in Table 1.

We have considered several dimensions of grids 6x11, 12x20 and 36x60 elements, with a 7.5 m high wall and a width of ground in front and behind equal to the height of the wall and the same for the substratum. Displacements are calculated by program (FLAC) for the most critical element. We have taken the grid 12x20 for the calculations which follow, since it gives reliable results with minimal computing time.

Table 1

Input data for numerical simulation

Characteristics of the ground	Characteristics of the metallic strip	Characteristics of the interface/strip
γ =1600 Kg/m^3 φ =36° K =1.6 E^7 N/m² G = 1E^7 N/m²	Number of bands (strips) per unit of width = 1 Width of calculation = 0.75m Width of the reinforcement = 0.04m Thickness of the reinforcement = 0.005m Modulus of elasticity of the strip = 200E^9 N/m² Maximum tensile force of the strip = 24000 N/m	The rigidity of shearing [N/m/m] = 1E^7. Initial coefficient of apparent friction = 1.5 Minimal coefficient of apparent friction = 0.72

5. Parametric studies

Comparative parametric studies were carried out between the traditional ultimate equilibrium method and the numerical method (FLAC) by varying the soil characteristics and various geometrical dimensions to delimit the critical plan of failure. The software FLAC^{2d} gives contours of shearing forces and displacements which make it possible to estimate the line or surface of failure. For each studied case, we have determined critical geometries of the three analytical models, the field of shearing determined by the FLAC software, the maximum axial force in the reinforcement and safety factors against breaking failure of the reinforcement and loss of adherence (pullout). These studies were carried out for various cases (six cases) in the same way, by varying each time the height of the wall H and the internal friction angle φ.

Case 1 : $H = 7.5$ m, $\varphi = 36°$

Fig. 4 represents the three failure surfaces (plane, circular and mixed) obtained by analytical calculation. The width of the upper part of the failure edge is different in the three models (Fig. 4). The model of mixed failure gives the smallest failure edge, whose highest width is equal to 0.356 H (2.67 m) and the height of vertical failure surface is equal to 0.25 H (1.875 m).

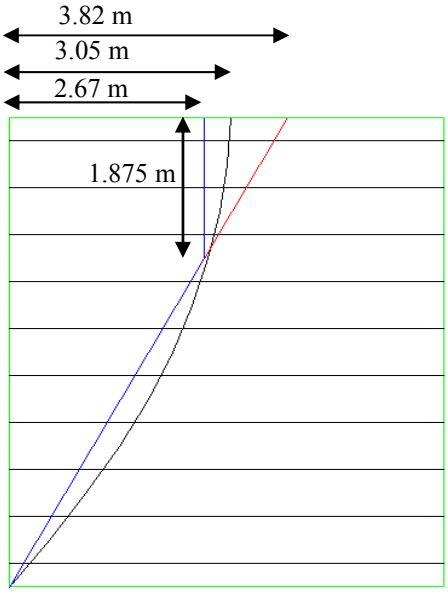

Fig. 4 Critical failure surfaces (Case 1)

The field of shearing represented in Fig. 5 gives a failure surface which has a form nearer to the model of mixed failure.

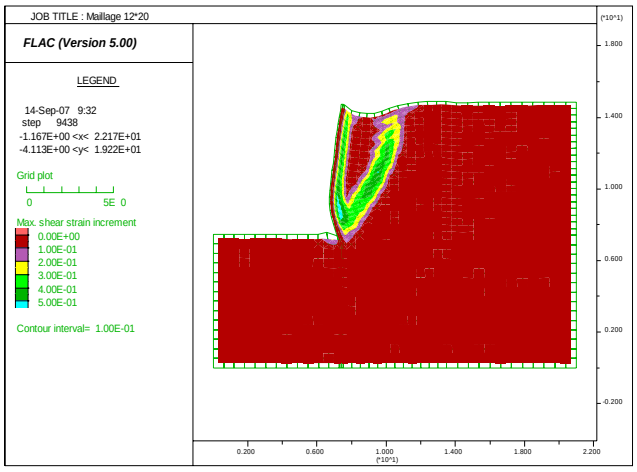

Fig. 5 Field of shearing indicating failure surface (Case 1)

Fig. 6 gives the maximum axial force in the reinforcement for each level of the wall for all the models studied. All models give the same results in the vicinity of medium of the wall. The model of circular failure gives the smallest tensile forces along the wall, except for the lower strip where the model of FLAC gives the smallest force. In general, the model of FLAC gives the greatest tension forces in the strips at all levels. The analytical model of mixed failure with bilinear and elliptic pressures is closer to the FLAC model.

According to Table 2 the model of mixed failure with elliptic pressure gives the smallest safety factors against breaking failure and lack of bond of the reinforcements compared to the other analytical models. This confirms that in this case, the model of mixed failure with elliptic pressure is the most unfavourable.

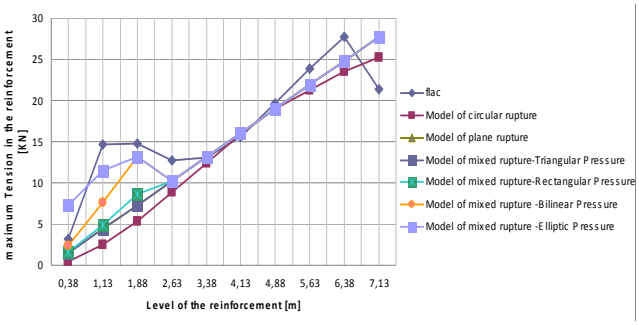

Fig. 6 Maximum axial force in the reinforcement on each level (Case 1)

Case 2 : $H = 7.5$ m, $\varphi = 30°$

In the 2nd case we keep the same parameters as in case 1 with a change only of the internal friction angle. The results obtained show that the model of mixed failure is the most unfavourable model with the slope of failure surface slightly softer than in the 1st case.

The curve of tensile forces of the model of mixed failure with elliptic pressure coincides well with the curve of tensile forces due to Flac which gives the greater forces (Fig. 7).

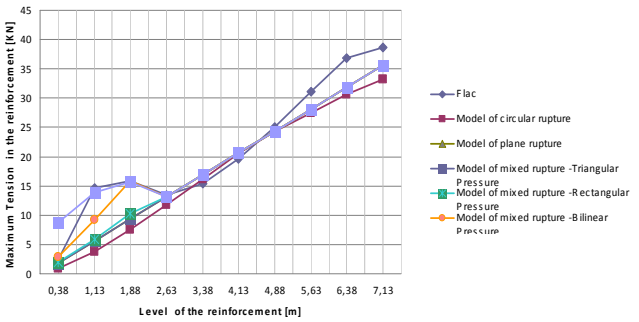

Fig. 7 Maximum axial force in the reinforcement on each level (Case 2)

According to Table 3 the model of mixed failure with elliptic pressure is the most dangerous model by giving the smallest safety factors.

The reduction of φ from 36° to 30° for the same height of wall leads to the reduction in safety factors (compare Tables 2 and 3) and an increase in tensile forces in the reinforcements (Figs. 6 and 7).

Case 3 : $H = 6$ m, $\varphi = 36°$

According to the results represented hereafter for a reinforced earth wall of height $H = 6$ and for an internal friction angle of 36° we can note that:

- the maximum tension force in the reinforcement is increasingly larger in the lower part of the wall than that in the upper part (Fig. 8);
- the delimitation of the field of shearing given by

FLAC^{2d} is closer to the model of mixed failure;

- the curve of the maximum tension forces according to FLAC^{2d} gives lower values compared to the other analytical models. The model of mixed failure gives the greatest tension forces in the reinforcements and particularly on the upper level of the wall (Fig. 8);
- according to Table 4 the model of mixed failure with elliptic pressure is the most unfavourable model.

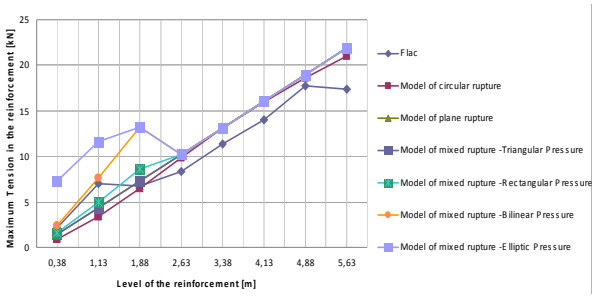

Fig. 8 Maximum axial force in the reinforcement on each level (Case 3)

Table 2

Safety factors obtained by various failure models (Case 1)

Safety factor	Failure Models					
	circular	plane	Mixed			
			Triangular pressure	Rectangular pressure	Bilinear pressure	Elliptic pressure
Fs_r	1.85	1.71	1.71	1.68	1.60	1.51
Fs_f	1.42	1.38	1.40	1.38	1.31	1.24

Table 3

Safety factors obtained by various failure models (Case 2)

Safety factor	Failure Models					
	circular	plane	Mixed			
			Triangular Pressure	Rectangular Pressure	Bilinear pressure	Elliptic pressure
Fs_r	1.41	1.33	1.33	1.32	1.25	1.19
Fs_f	0.87	0.87	0.88	0.88	0.83	0.79

Table 4

Safety factors obtained by various failure models (Case 3)

Safety factors	Failure Models					
	circular	Plane	Mixed			
			Triangular Pressure	Rectangular Pressure	Bilinear pressure	Elliptic pressure
Fs_r	2.23	2.13	2.13	2.09	1.93	1.77
Fs_f	1.25	1.23	1.26	1.23	1.14	1.05

Table 5

Safety factors obtained by various failure models (Case 5)

Safety factor	Failure Models					
	circular	plane	Mixed			
			Triangular Pressure	Rectangular Pressure	Bilinear pressure	Elliptic pressure
Fs_r	1.59	1.42	1.42	1.39	1.30	1.21
Fs_f	1.67	1.57	1.60	1.57	1.47	1.36

Case 4 : $H = 6$ m, $\varphi = 30°$

In this case the change of internal angle of friction has an effect on the slope of failure surfaces, and the model of mixed failure with elliptic pressure is the most unfavourable by giving the greatest tension forces in the reinforcements and the smallest factors of safety.

Case 5 : $H = 9$ m, $\varphi = 36°$

The model of mixed failure according to Fig. 9 and Table 5 is the most critical model, with a width of the wedge of 0.33 H and vertical height of 0.29 H. The model of mixed failure with elliptic pressure gives the greatest tensile forces (Fig. 10).

Case 6: $H = 9$ m, $\varphi = 30°$

We note from the results the influence of the variation of internal friction angle on the slope of the failure surfaces. The model of mixed failure remains always the most critical model amongst all the models studied including that of FLAC.

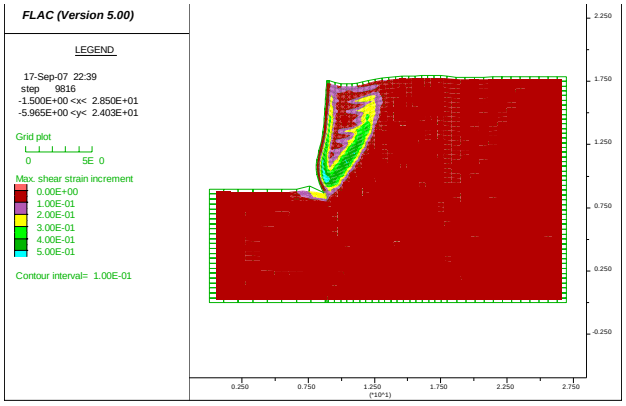

Fig. 9 Field of shearing indicating failure surface (case 5)

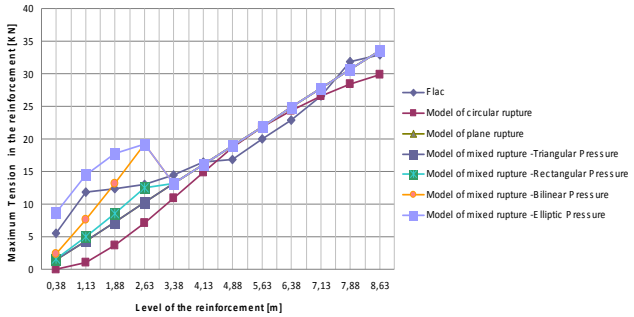

Fig. 10 Maximum axial force in the reinforcement on each level (case 5)

In conclusion the comparative analysis of the results obtained enabled us to make these important observations:

- the most critical failure model is generally the mixed failure model with elliptic distribution of pressures of the ground behind the vertical failure surface;
- the fields of shearing given by software FLAC^{2d} delimit failure contour which is very often close to the mixed failure model;
- the maximum displacement in the reinforced earth walls by failure is obtained at the base of the wall and gives greater tensile forces at this level. Therefore for pre-dimensioning of the reinforcements, we take the force of the last strip by taking account of the results of the tests;
- height of the wall and internal friction angle have an effect on the geometry of the failure models (slope of the failure surfaces) and tensile forces in the reinforcements;
- the internal friction angle and the height of the wall influence widely the safety factors against breaking failure and lack of bond of the reinforcements. Reduction in the internal friction angle led to a reduction in the two safety factors because of the decrease of the friction ground-strip. The increase of the height of the wall decreases the first and increases the second.

6. Conclusions

In this paper we have studied internal stability of the reinforced earth retaining walls by traditional limit equilibrium method and numerical methods using FLAC^{2d} software. The objective of this paper is to find the most dangerous (unfavourable) overall failure model "facing-ground-reinforcement" by reinforced earth retaining walls. A detailed parametric study by varying geometrical parameters of the wall and parameters of the ground (internal friction angle) was carried out. Comparative analysis of the results enabled us to obtain a useful knowledge. The most critical failure model is generally the model of mixed failure. The fields of shearing given by software FLAC^{2d} delimit a contour which is very often close to the model of mixed failure.

References

1. **Elias, V., Christopher, B.R., Berg, R.R.** Mechanically Stabilized Earth Walls and Reinforced Soil Slopes. Design & Construction Guidelines. Federal Highway Administration, Report N°FHWA-NHI-00-043, 2001. -394p.
2. **Robert, D.H., Wei, F.L.** Internal Stability Analyses of Geosynthetic Reinforced Retaining Walls. -Washington state transportation center (TRAC), 2002.-465p.
3. Les ouvrages en Terre Armée : recommandations et règles de l'art. Laboratoire Central des Ponts et Chaussées, Paris, 1991.-189p.
4. **Chen, W.F., Han, D.J.** Plasticity for Structural Engineers. -New York: -Springer-Verlag, 1988.-606p.
5. **Unterreiner, P., Schlosser, F.** Renforcement des sols par inclusions. -Techniques de l'ingénieur, 1994.-19p.
6. **Frantová, M.** Modification of Chen model of plasticity for early ages applications.-Mechanika.-Kaunas: Technologija, 2006, Nr.2(58), p.11-16.
7. **Dabkevičius, A., Kibirkštis, E.** Investigation of mechanical characteristics of polymer films for packaging production. -Mechanika. -Kaunas: Technologija, 2006, Nr4(60), p.5-8.
8. Note of the software FLAC ITASCA Consulting Group. INC, Minneapolis, Minnesota, 2002.-82p.

L. Belabed, J. Yahiaoui, A.M. Zennir, H. Benyaghla

SUSTIPRINTO GRUNTO ATRAMINIŲ SIENELIŲ MECHANINĖ ELGSENA

R e z i u m e

Šlaitų stabilizavimas, sustiprinant gruntą (Terre Armée), yra labai konkurencinga technologija (ekonomiška ir patikima). Remiantis teoriniais ir eksperimentiniais tyrimais, straipsnyje siūloma sustiprinto grunto atraminių sienelių bendrąjį vidinį stabilumą tikrinti remiantis trimis mechaniniais modeliais, analitiniu ribinės pusiausvyros (funkcionavimo sutrikimo) metodu. Šio straipsnio pagrindinis tikslas – palyginti minėtų mechaninių modelių funkcionavimo sutrikimus su sutrikimais, nustatytais skaitmenine analize (FLAC^{2d} kodas), kartu įteisinant kiek galima realesnius nepageidaujamus modelio funkcionavimo sutrikimus. Atlikti parametriniai ir lyginamieji tyrimai suteikė naudingų žinių, susijusių su sustiprinto grunto atraminių sienelių vidiniu stabilumu, ir leido pasiūlyti skaičiavimams teorinį modelį, grindžiamą bandymais patvirtintu skaitmeniniu modeliavimu.

L. Belabed, J. Yahiaoui, A.M. Zennir, H. Benyaghla

MECHANICAL BEHAVIOUR OF REINFORCED EARTH RETAINING WALLS

S u m m a r y

Stabilization of the slopes by the technique of reinforced earth (Terre Armée) is a very concurrent technique (economical and reliable). Based on the results of theoretical and experimental studies, we propose in this paper to check the overall internal stability of reinforced earth retaining walls by three mechanical models, using the analytical method of the limit equilibrium (failure). The main objective of this paper is to compare these failure mechanical models with the failure models obtained by numerical analysis (code FLAC^{2d}), in order to validate the most realistic and more unfavourable failure models. Parametric and comparative studies carried out have allowed us to bring a very useful knowledge concerning the study of internal stability of the reinforced earth retaining walls and to propose a theoretical mechanical model of calculation proven by numerical simulation and confirmed by tests.

Л. Белабед, Й. Иагиаоуи, А.М. Зеннир, Г. Бениаггла

МЕХАНИЧЕСКОЕ ПОВЕДЕНИЕ ПОДПОРНОЙ СТЕНКИ ИЗГОТОВЛЕННОЙ ИЗ УКРЕПЛЕННОГО ГРУНТА

Р е з ю м е

Стабилизация склонов используя технологию укрепленного грунта является конкурентной технологией (она экономична и надежна). Основываясь на теоретические и экспериментальные исследования в статье предлагается общую внутреннюю устойчивость подпорной стенки, изготовленной из укрепленного грунта, проверять тремя реальными механическими моделями применяя аналитический метод предельной устойчивости. Основная цель этой работы – сравнить нарушение функциональности упомянутых механических моделей с нарушениями, установленными при использовании цифрового анализа (код FLAC^{2d}) и при этом узаконить возможно реалистические и негативные срывы функционирования модели. Выполненные параметрические и сравнительные исследования позволили получить полезные данные по отношению стабильности подпорной стенки, изготовленной из укрепленного грунта, и предложить для расчетов подтвержденный экспериментами метод численного моделирования созданной теоретической модели.

Received December 22, 2008
Accepted February 05, 2009